Geophysical Research Letters

RESEARCH LETTER
10.1029/2021GL096838

Efficient Production of Carbonyl Sulfide in the Low-NO_x Oxidation of Dimethyl Sulfide

Christopher M. Jernigan[1], Charles H. Fite[2], Luc Vereecken[3], Max B. Berkelhammer[4], Andrew W. Rollins[5], Pamela S. Rickly[5,6], Anna Novelli[3], Domenico Taraborrelli[3], Christopher D. Holmes[2], and Timothy H. Bertram[1]

[1]Department of Chemistry, University of Wisconsin-Madison, Madison, WI, USA, [2]Department of Earth, Ocean and Atmospheric Science, Florida State University, Tallahassee, FL, USA, [3]Institute of Energy and Climate Research, Troposphere (IEK-8), Forschungszentrum Jülich GmbH, Jülich, Germany, [4]Department of Earth and Environmental Sciences, University of Illinois at Chicago, Chicago, IL, USA, [5]NOAA Chemical Sciences Laboratory, Boulder, CO, USA, [6]Cooperative Institute for Research in Environmental Sciences, University of Colorado, Boulder, CO, USA

Key Points:

- Carbonyl sulfide (OCS) is formed in the OH-oxidation of dimethyl sulfide (DMS) under conditions relevant to the marine boundary layer
- The multi-generational OCS production proceeds through soluble, stable intermediates making it sensitive to multiphase, cloud chemistry
- Implementing a new DMS oxidation mechanism in a global chemical transport model yields a more robust depiction of DMS-derived OCS production

Supporting Information:

Supporting Information may be found in the online version of this article.

Correspondence to:

T. H. Bertram,
timothy.bertram@wisc.edu

Citation:

Jernigan, C. M., Fite, C. H., Vereecken, L., Berkelhammer, M. B., Rollins, A. W., Rickly, P. S., et al. (2022). Efficient production of carbonyl sulfide in the low-NO_x oxidation of dimethyl sulfide. *Geophysical Research Letters*, *49*, e2021GL096838. https://doi.org/10.1029/2021GL096838

Received 9 NOV 2021
Accepted 14 JAN 2022

Author Contributions:

Conceptualization: Luc Vereecken
Formal analysis: Charles H. Fite
Funding acquisition: Christopher D. Holmes
Investigation: Luc Vereecken
Methodology: Charles H. Fite, Luc Vereecken
Project Administration: Christopher D. Holmes
Resources: Luc Vereecken, Max B. Berkelhammer, Andrew W. Rollins, Pamela S. Rickly
Software: Charles H. Fite, Luc Vereecken, Anna Novelli, Domenico Taraborrelli, Christopher D. Holmes
Supervision: Christopher D. Holmes

Abstract

The oxidation of carbonyl sulfide (OCS) is the primary, continuous source of stratospheric sulfate aerosol particles, which can scatter shortwave radiation and catalyze heterogeneous reactions in the stratosphere. While it has been estimated that the oxidation of dimethyl sulfide (DMS), emitted from the surface ocean accounts for 8%–20% of the global OCS source, there is no existing DMS oxidation mechanism relevant to the marine atmosphere that is consistent with an OCS source of this magnitude. We describe new laboratory measurements and theoretical analyses of DMS oxidation that provide a mechanistic description for OCS production from hydroperoxymethyl thioformate, a ubiquitous, soluble DMS oxidation product. We incorporate this chemical mechanism into a global chemical transport model, showing that OCS production from DMS is a factor of 3 smaller than current estimates, displays a maximum in the tropics consistent with field observations and is sensitive to multiphase cloud chemistry.

Plain Language Summary

Accurate estimates of marine carbonyl sulfide (OCS) sources are critical for both modeling stratospheric aerosol concentrations, as OCS is an important precursor to stratospheric sulphate aerosol particles, and for estimating gross primary production, as OCS is readily consumed by the terrestrial biosphere. Despite the importance of OCS to both stratospheric aerosol chemistry and as an effective proxy for CO_2 plant uptake, considerable uncertainty remains in the sources and sinks of OCS. A large source of this uncertainty arises in the marine sources, dominated by the oxidation of marine sulfur gases. Here, we examine the global production of OCS from the oxidation of a marine biologically produced molecule, dimethyl sulfide (DMS). We show that the multi-generational production of OCS proceeds through the oxidation of stable, water-soluble intermediates. Using a global chemical transport model, we find that OCS production is largest in the tropics, where cloud loss of hydroperoxymethyl thioformate, the primary precursor to OCS in the DMS oxidation mechanism, is at a minimum.

1. Introduction

Carbonyl sulfide (OCS) is the most abundant sulfur-containing gas in Earth's atmosphere with an estimated lifetime of greater than 2 years (Brühl et al., 2012; Chin & Davis, 1993; Montzka et al., 2007). In the stratosphere, OCS is a principle precursor to sulfate aerosol which plays a critical role in Earth's radiation budget and can serve to catalyze heterogeneous reactions with importance to stratospheric ozone chemistry (Crutzen, 1976; Solomon et al., 1986). In the troposphere, OCS is readily consumed by the terrestrial biosphere, and has proven to be an effective tool for estimating gross primary production (GPP; Asaf et al., 2013).

Despite the importance of OCS to stratospheric chemistry and its utility for estimating GPP, the magnitude and spatial distribution of OCS sources remain poorly constrained (Kremser et al., 2016; Ma et al., 2021). It has been shown that OCS is directly emitted to the atmosphere from oceans (Von Hobe et al., 2001), wetlands (Watts, 2000), and anoxic soils (Devai & DeLaune, 1995), is formed chemically in the atmosphere through the oxidation of dimethyl sulfide (DMS; Barnes et al., 1994) and carbon disulfide (CS_2; Chin & Davis, 1993), and is released through a wide variety of anthropogenic activities (Zumkehr et al., 2018).

Validation: Charles H. Fite, Luc Vereecken, Anna Novelli, Domenico Taraborrelli, Christopher D. Holmes
Writing – review & editing: Charles H. Fite, Luc Vereecken, Max B. Berkelhammer, Andrew W. Rollins, Pamela S. Rickly, Anna Novelli, Domenico Taraborrelli, Christopher D. Holmes

Recent isotopic and inverse modeling studies indicate that the marine environment is the dominant source region for OCS and that there is either an over-estimation of the terrestrial OCS sink or an unaccounted-for OCS source that seems to be centered in the tropical oceans based on atmospheric inversion studies (Berry et al., 2013; Davidson et al., 2021; Ma et al., 2021). In response to recent suggestions that the production of OCS from the OH-initiated oxidation of DMS may be a significant source of uncertainty in the OCS budget (Davidson et al., 2021; Ma et al., 2021) and new discoveries of the chemical mechanism of DMS oxidation (Berndt et al., 2019; G. A. Novak et al., 2021; Veres et al., 2020; Wu et al., 2015), we revisit here the chemical mechanism for OCS production in the oxidation of DMS.

Most existing global OCS emission inventories use a uniform yield (0.7%) to calculate OCS production (P_{OCS}) from DMS ocean emissions (E_{DMS}; i.e., for E_{DMS} = 22 TgS yr^{-1}, P_{OCS} = 0.155 TgS yr^{-1}; e.g., Kettle et al., 2002). The OCS yield from the OH-initiated oxidation of DMS originates from the early laboratory studies of Barnes et al. (1994) where the production of OCS was attributed to the photo-oxidation of thioformaldehyde (H_2CS), a product of peroxy radical (RO_2•) bimolecular chemistry (Figure 1)**.** Due to limitations in the analytical techniques available at the time, it was necessary to conduct these experiments at high precursor concentrations which are not representative of typical marine conditions. The experimental conditions resulted in large RO_2• concentrations that over-emphasized bimolecular chemistry (RO_2•+RO_2•), thus shortening the lifetime of RO_2• ($\tau(RO_2\bullet)_{bimol}$ < 5 s) at the expense of isomerization chemistry that is expected to dominate under pristine marine conditions. Recently, it has been shown that the methylthiomethyl peroxy radical radical (MTMP, $CH_3SCH_2O_2$•), the primary peroxy radical formed following H-abstraction of DMS, efficiently isomerizes to a stable intermediate, hydroperoxymethyl thioformate (HPMTF, $HOOCH_2SCH = O$) which has been observed to be ubiquitous in marine environments (Berndt et al., 2019; Veres et al., 2020; Vermeuel et al., 2020; Wu et al., 2015; Ye et al., 2021). Given the key role of unimolecular isomerization and secondary chemistry in the oxidation of DMS, that was suppressed in previous experiments, it is essential to revisit the formation of OCS under conditions (i.e., $\tau(RO_2\bullet)_{bimol}$ > 100 s) that accurately represent the marine environment.

Here, we present laboratory measurements of DMS oxidation conducted under dark, low RO_2 and NO_x-free conditions to determine the oxidation mechanism and reaction intermediates in the chemical trajectory that connects DMS emissions with OCS formation. Our experiments, supported by new quantum chemical and theoretical kinetic calculations on the extended HPMTF chemistry, show that OCS is formed in high yield in the OH oxidation of HPMTF. These results underscore that modeling global OCS formation from DMS oxidation as a single fixed yield is inconsistent with the current understanding of DMS oxidation chemistry that proceeds through several stable, soluble intermediates and their specific chemistry including removal via multiphase processes (Hoffmann et al., 2016; G. A. Novak et al., 2021; Veres et al., 2020). We incorporate a simplified version of the chemical mechanism developed here into a global chemical transport model to quantify P_{OCS} and its response to HPMTF cloud chemistry that sequesters HPMTF and limits P_{OCS} in the cloudy marine boundary layer. We show that the multiphase and chemical mechanism-based approach results in a lower OCS global production rate with a spatial and temporal emission pattern different from the fixed-yield approach.

2. Methods

Detection and quantification of trace gases was conducted using two Chemical Ionization Mass Spectrometers (CIMS), an Aerodyne Compact Time of Flight CIMS (C-ToF) utilizing iodine ion chemistry (Bertram et al., 2011) and an Aerodyne/TOFWERK Vocus - Proton Transfer Reaction Time of Flight Mass Spectrometer (Vocus; J. Krechmer et al., 2018). A custom-built laser-induced fluorescence (LIF) spectrometer (Rickly et al., 2021; Rollins et al., 2016) and a Los Gatos Research Enhanced Performance OCS analyzer (Berkelhammer et al., 2016) were used to detect sulfur dioxide (SO_2) and OCS, respectively. DMS and methane thiol (MeSH), used for instrument calibrations and the environmental chamber experiments, were supplied from compressed gas cylinders (Praxair, DMS at 5.08 ppm in N_2 and Airgas, MeSH at 6.11 ppm in N_2) diluted to the target concentration. The sensitivity of the C-ToF toward HPMTF was determined to be 5 ncps pptv^{-1} using a flow reactor experiment previously described in Supporting Information S1 of Vermeuel et al. (2020) and was further verified by sulfur mass balance in the environmental chamber. For molecules identified in the Iodine CIMS mass spectrum, where commercially available standards were not available, absolute sensitivities were determined using the calculated binding enthalpy to iodine as described in Iyer et al. (2016). Species identified in the Vocus—PTR mass spectrum, where commercially available standards were not available, were assigned absolute sensitivities

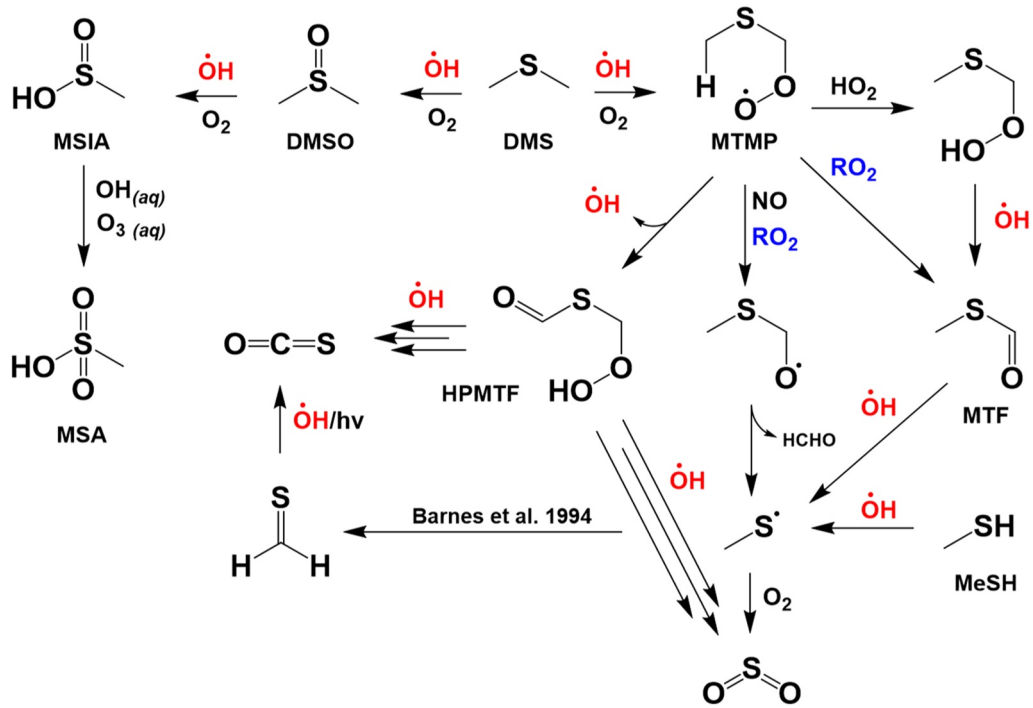

Figure 1. Chemical mechanism for the gas-phase OH-oxidation of dimethyl sulfide. Simplified chemical mechanism for the production of carbonyl sulfide (OCS) in the gas-phase OH-oxidation of dimethyl sulfide and methanethiol. The mechanism shown here combines the work of Barnes et al. (1994) and the hydroperoxymethyl thioformate (HPMTF)-derived OCS production pathway proposed here. The triplicate arrows pointing away from HPMTF denote multi-step mechanisms addressed in Supporting Information S1.

by relating their literature proton affinity to those of species calibrated by liquid or cylinder methods (e.g., DMS, DMSO, acetone, and TME). Limits of detection (LOD) of HPMTF and OCS were determined to be 0.53 pptv and 2.21 pptv following the method of Bertram et al. (2011), at an integration time of 25 and 300 s, respectively. Chamber experiments were run in a 0.6 m^3 5 mil (mil, 0.001 of an inch) PFA environmental chamber under ambient temperature (298 ± 1 K) and low relative humidity (<0.5% RH). The theoretical study is based on quantum chemical calculations at the CCSD(T)/aug-cc-pV(Q+d)Z//M06-2X-D3/aug-cc-pV(T+d)Z level of theory, combined with transition state theory and RRKM-master equation calculations incorporating all conformers. Detailed discussion of the experimental and theoretical methods can be found in Supporting Information S1.

3. Production of OCS in the Low-NO_x Oxidation of DMS

To investigate the mechanism for OCS production from DMS under typical marine conditions, we conducted a series of dark, continuous flow environmental chamber experiments focused on the OH-initiated oxidation of DMS. Experiments were conducted at oxidant concentrations representative of the pristine marine environment ($[HO_x] \equiv [HO_2\bullet] + [\bullet OH]$ and $[NO_x] \equiv [NO] + [NO_2]$ <10 pptv $[RO_2\bullet]$ < 150 ppt and $\tau(CH_3SCH_2O_2\bullet)_{bimol}$ > 100 s; Creasey et al., 2003; Lee et al., 2009; Vaughan et al., 2012). Hydroxyl radicals (•OH) were generated by the ozonolysis of tetramethyl ethylene (TME). Dry synthetic air conditions (<0.5% RH, 80% N_2/20% O_2) were used to facilitate higher yields of •OH from TME ozonolysis (Y_{OH} > 0.8) and to mitigate chamber wall losses (Alam et al., 2013; Donahue et al., 1998).

In our experiments, we observe consistent and reproducible ($N = 7$) production of OCS in the OH-oxidation of DMS under oxidative conditions representative of the pristine marine atmosphere (Figure 2a). As discussed below, OCS production in our experiment cannot be attributed solely to the photo-oxidation of H_2CS as previously suggested or experimental artifacts (Figure 1). We stress that the absolute fraction of OCS formed from DMS in this or any chamber study is specific to the experimental conditions of the environmental chamber (e.g., the fraction of second generation products that are oxidized) and not directly applicable to all atmospheric conditions

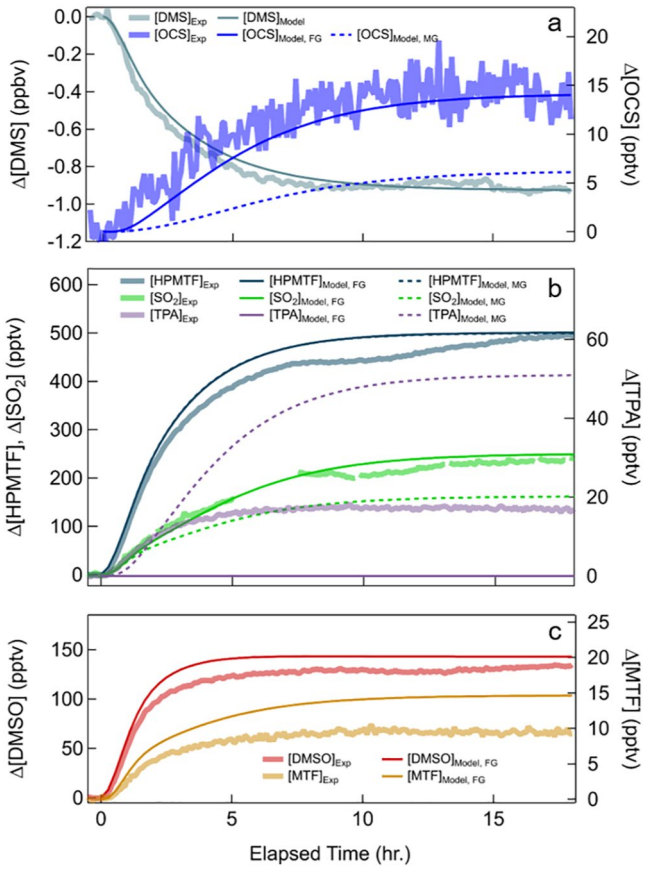

Figure 2. Laboratory measurements of carbonyl sulfide (OCS) production from the OH-oxidation of dimethyl sulfide (DMS). Measurements (translucent thick lines) and first generational (FG, solid thin lines) and multi-generational (MG, dashed thin lines) model calculations of S-containing reaction products of the OH-oxidation of DMS. Measurements were conducted in an environmental chamber under low NO_x oxidation conditions. Reaction products include: (OCS), hydroperoxymethyl thioformate, sulfur dioxide, thioperformic acid, methyl thioformate, and dimethyl sulfoxide.

as P_{OCS} from DMS oxidation is a function of: (a) the temperature-dependent fraction of DMS that is oxidized to MTMP, (b) the fraction of MTMP that forms HPMTF, a function of the temperature-dependent MTMP isomerization rate (NO), (HO_2•), and (RO_2•) and (c) the fraction of HPMTF that is lost to chemical reaction with OH, which we suggest to be the dominant pathway for the gas-phase production of OCS from DMS. It has also been suggested that photolysis of the peroxide group in HPMTF could lead to OCS formation (Khan et al., 2021). To generalize the experiments described here, we use a chemical box model constrained by experimental observations and theoretical kinetic calculations to examine the chemical mechanism that leads to OCS formation in the OH-oxidation of DMS and develop a simplified mechanistic model for OCS production that can be incorporated into global chemical transport models to more accurately describe DMS-derived OCS production.

4. Chemical Mechanism for OCS Production in the OH-Oxidation of DMS

We examined three possible gas-phase pathways for OCS formation from DMS in our experiments: (a) OH-oxidation of H_2CS, a product of MTMP bimolecular chemistry, (b) direct OCS formation from the OH-oxidation of HPMTF, a product of MTMP isomerization, and (c) OCS production from the oxidation of stable products of HPMTF OH-oxidation, such as thioformic anhydride (TFA) and thioperformic acid (TPA).

The production of OCS from the oxidation of H_2CS was originally suggested by Barnes et al. (1994), where H_2CS was proposed to be formed in the reaction of the methylthiyl (CH_3S•) radical and O_2, where CH_3S• is a prompt product of the reaction of MTMP with HO_2, RO_2, or NO (Barnes et al., 1996; Mardyukov & Schreiner, 2018; Yin, Grosjean, Flagan, & Seinfeld, 1990). To evaluate the potential for the OH-oxidation of CH_3S• to produce OCS, we examined the OH-oxidation of methane thiol (MeSH) as this reaction proceeds predominantly via H-abstraction leading to prompt and near unit yield of CH_3S•, providing a clean test for the production of OCS from MTMP bimolecular chemistry. In the MeSH experiments, also conducted under low NO_x and RO_2• conditions, no OCS production was observed (Figure S6 in Supporting Information S1) indicating that the OCS observed in the DMS experiment is not formed through MTMP bimolecular chemistry. This is supported by the work of Chen et al. (2021), who also found that CH_3S• oxidizes to SO_2 in near unit yield and not H_2CS, a potential precursor to OCS.

The first-generation production of OCS from the OH-oxidation of HPMTF has only been studied theoretically, where the thermal OCS yield was previously calculated to be insignificant (<0.01%; Wu et al., 2015). Here we revisit the production of OCS in the OH-oxidation of HPMTF using both experimental and theoretical tools. We first determine the rate constant for HPMTF + OH ($k_{HPMTF + OH}$), a key fundamental step that connects DMS and OCS, using a 0-D box model that incorporates the Master Chemical Mechanism (MCM) v3.3.1 in the Framework for 0-D Atmospheric Modeling (F0AM; M. E. Jenkin et al., 1997; Saunders et al., 2003; Wolfe et al., 2016), constrained by chamber observations. In addition to the measurements of [HPMTF], we use measurements of dimethyl sulfoxide (DMSO) to constrain the fraction of DMS lost to the OH-addition channel (41%, consistent with known kinetics), methyl thioformate (MTF) to determine the RO_2 concentration and MTMP bimolecular reaction rates (see in Supporting Information S1 for more information), and OCS and SO_2 to constrain the terminal products of DMS oxidation within the model (Figures 2b and 2c). HPMTF production and loss rates were added to the existing MCM DMS oxidation mechanism and optimized to match observations, as discussed below. HPMTF production from MTMP involves a two-step isomerization mechanism that is rate-limited by the first H-shift (k_{isom}) that has been both calculated theoretically ($k_{isom, Veres}$ (293 K) = 0.041 s^{-1}, $k_{isom, Wu}$ (293 K) = 2.1 s^{-1}; Veres et al., 2020; Wu et al., 2015) and experimentally determined ($k_{isom, Berndt}$ (295 K) = 0.23 ± 0.12 s^{-1}, $k_{isom, Ye}$ (293 K) = 0.09

(0.03–0.3) s^{-1}, $k_{isom,\ this\ study}$ (298 K) = 0.1 ± 0.05 s^{-1}; Berndt et al., 2019; Ye et al., 2021). To determine $k_{HPMTF+OH}$ from the constrained box-model, we set k_{isom} = 0.1 s^{-1}. HPMTF loss is driven by: (a) gas-phase reaction with OH ($k_{HPMTF+OH}$), (b) wall loss processes, and (c) chamber dilution intrinsic to a continuous flow regime. Using the box-model, constrained by the HPMTF growth curve and steady state concentration, and concentrations of other known sulfur species (DMS, DMSO, MTF, SO_2), $k_{HPMTF+OH}$ was determined to be 1.4 (0.27–2.4) × 10^{-11} cm^3 $molec^{-1}$ s^{-1}, where the range in $k_{HPMTF+OH}$ is based on propagation of all sources of systematic uncertainty in the experiment (in Supporting Information S1). The experimentally determined rate ($k_{HPMTF+OH}$) is an order of magnitude faster than the theoretical rate originally proposed by Wu et al. (2015), but within uncertainty of the experimentally-determined rate for the structurally similar molecule, methyl thioformate (k_{MTF+OH} = 1.11 ± 0.2 2 × 10^{-11} cm^3 $molec^{-1}s^{-1}$) and the theoretical rate determined in this study ($k_{HPMTF+OH}$ (298K) = 0.68 × 10^{-11} cm^3 $molec^{-1}$ s^{-1}). Additional chamber experiments performed to isolate the isomerization rate, HPMTF + OH loss rate, the sulfur product distribution, and model description are discussed in the SI.

In the OH-oxidation of HPMTF, we suggest that OCS can be formed as either a direct, first-generation product of HPMTF + OH, proceeding from the H-abstraction of the aldehydic hydrogen and the prompt decomposition of $HOOCH_2SC=O$ or as a multi-generational product following the OH-oxidation of the HPMTF reaction products thioformic anhydride (TFA, CHOSCHO) or thioperformic acid (TPA, HC(=S)OOH).

We first treat OCS formation empirically, using a simplified model where we determine the net OCS branching fraction from HPMTF+ OH (ϕ_{OCS} = 13%) required to sustain the measured OCS (Figure 2a). Uncertainty in the determination of ϕ_{OCS} (8.5% < ϕ_{OCS} < 49%) is dependent on the accuracy of the MTMP isomerization rate (k_{isom}) used to determine $k_{HPMTF+OH}$ (see in Supporting Information S1). This analysis simplifies the chemical mechanism for inclusion in global models but does not permit correct accounting for multi-generational OCS production from TFA or TPA.

To further examine the multi-generational OH-oxidation of HPMTF, we also developed an extensive temperature dependent mechanistic framework for HPMTF oxidation to OCS based on theoretical kinetic calculations (SI 8, 9). Results from the multi-generational mechanistic model are also shown in Figure 2, where modeled steady-state (OCS) agrees to within a factor of two of the experimental measurement and a mechanistic pathway to describe the formation of TPA, observed in our study, is introduced. The pure theory-based multi-generation model does well to describe (OCS) and the existence of TPA, but additional chemistry or optimizations need to be introduced to fully capture the prompt formation of OCS and TPA, and the yield of SO_2 (Figure 2b). Remaining differences between the model prediction and the experiment could be due to reactions of the highly soluble intermediates occurring on the Teflon chamber walls, although these are expected to be suppressed due to the low relative humidity (<0.5%) and the omission of gas-phase reactions of ozone with radical intermediates (e.g., $HOOCH_2S\bullet + O_3$) in the theoretical mechanism. It is important to note here that the gas-phase production of OCS from DMS proceeds through three very soluble species (HPMTF, TFA and TPA), the condensed phase chemistry of which is currently unknown, and likely significantly modulates the production of OCS from DMS in regions with high aerosol surface area or cloud cover. A more detailed discussion of model-measurement uncertainty, limitations in $k_{HPMTF+OH}$ and ϕ_{OCS} and the theoretical HPMTF mechanism can be found in Supporting Information S1.

5. Global Estimates of OCS Production From DMS Oxidation

Global OCS production is modeled based on the simplified mechanism-based approach involving only first-generation HPMTF chemistry, that is, $P_{OCS} = \phi_{OCS} \times k_{OH+HPMTF}$[HPMTF][OH], where $k_{OH+HPMTF}$ is 1.4 × 10^{-11} cm^3 $molec^{-1}$ s^{-1} and ϕ_{OCS} = 13%. This approach is compared with the existing, fixed-yield model where $P_{OCS} = Y_{OCS} \times L_{DMS}$, Y_{OCS} = 0.7% and L_{DMS} is the loss rate of DMS to reaction with OH or k_{DMS+OH}[OH][DMS]. We used the GEOS-Chem global chemical transport model with an expanded DMS oxidation mechanism and model updates to halogen chemistry and cloud processing (Holmes et al., 2019; G. A. Novak et al., 2021; Veres et al., 2020; Wang et al., 2019, 2021; version 12.9.2, www.geos-chem.org, see in Supporting Information S1 for more details). As shown in Figure 3a, the mechanism-based approach for calculating P_{OCS} (shown in red) results in a dramatic increase in the OCS source term from DMS oxidation (P_{OCS} = 680.1 GgS yr^{-1}) compared with the traditional, fixed-yield approach (green line, P_{OCS} = 106.1 GgS yr^{-1}). In the fixed-yield case P_{OCS} directly tracks DMS and OH concentrations, with enhancements in the Southern Ocean (Lana

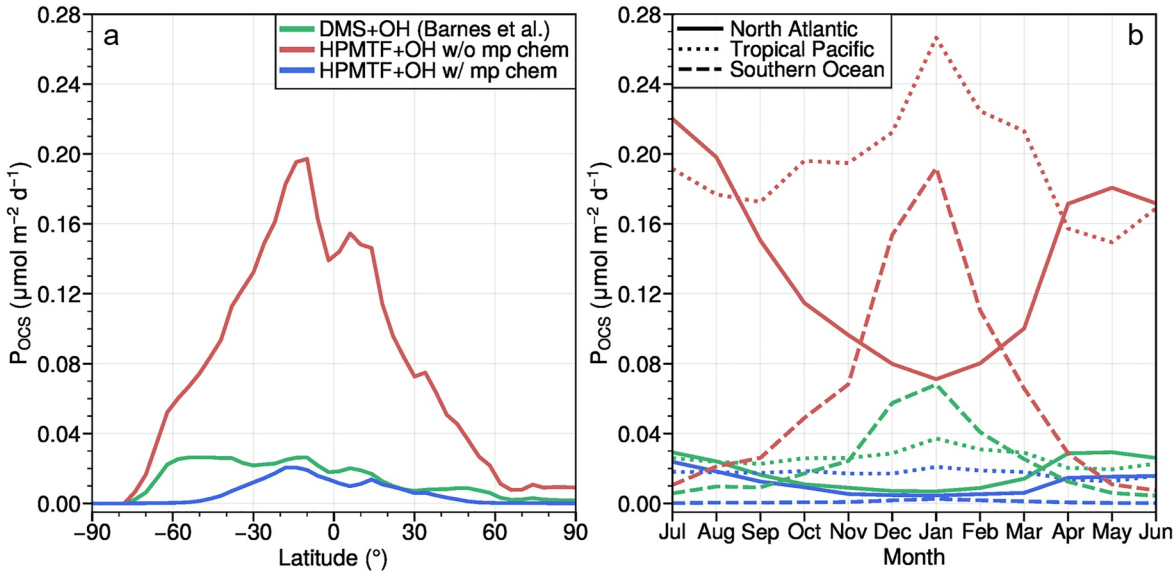

Figure 3. Modeled meridional and annual distribution of column carbonyl sulfide (OCS) production from the oxidation of di methyl sulfide (DMS). (a) Modeled meridional distribution of OCS production (P_{OCS}). The green trace depicts P_{OCS} calculated as a fixed yield (0.7%) of total DMS emission, the red and blue traces incorporate the HPMTF-based OCS production mechanism for an OCS branching fraction (ϕ_{OCS} = 13%) in the HPMTF + OH reaction with (blue) and without (red) multiphase chemistry. (b) Modeled annual distribution of P_{OCS} for three marine regions for each of the three model representations of P_{OCS} shown in panel a. A map defining the three marine regions is shown in Supporting Information S1 (Figure S23 in Supporting Information S1).

et al., 2011; Figures 4a and 4b). In contrast, results from the mechanism-based scenario indicate strong OCS production in the tropics that is associated with warmer temperatures that favor HPMTF formation and thus OCS production.

As noted above, it is well established that soluble molecules such as HPMTF are efficiently removed from the atmosphere via uptake to clouds and aerosol particles and through surface deposition. Vermeuel et al. (2020) and G. A. Novak et al. (2021), showed that cloud-loss can be a dominant sink for HPMTF in the marine boundary layer. In the context of the OCS budget, efficient cloud-loss of HPMTF likely terminates OCS production, setting

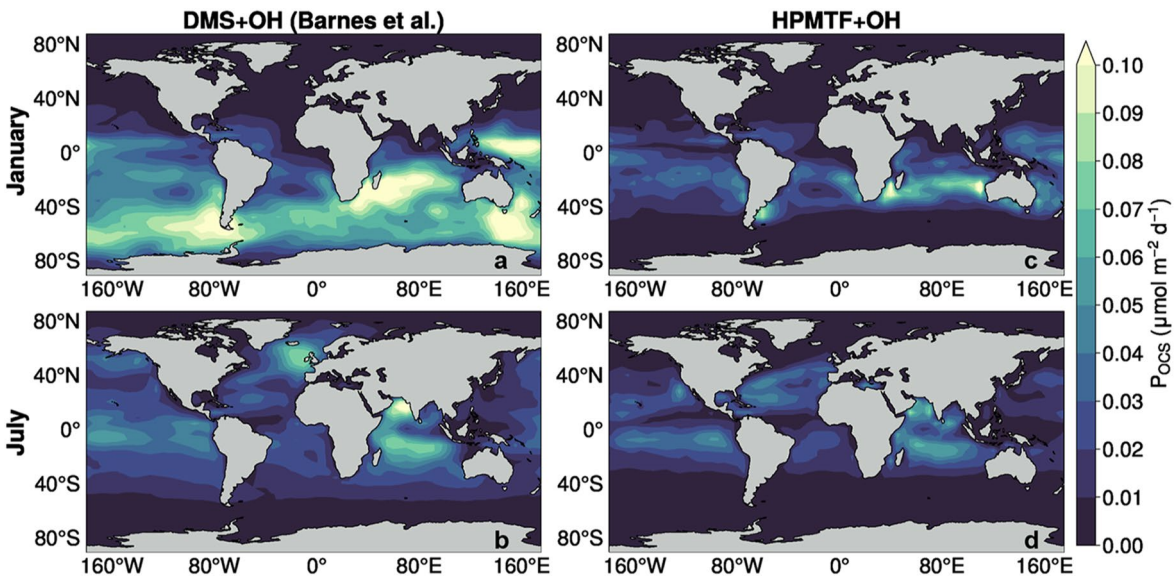

Figure 4. Global distribution of column carbonyl sulfide (OCS) production from the oxidation of DMS. Modeled global distribution of OCS production (P_{OCS}) calculated as a fixed yield (0.7%) of total DMS emission (a,b) and the HPMTF-based P_{OCS} mechanism at a ϕ_{OCS} of 13% with multiphase chemistry (c,d) during the month of January (b–d) and July (a–c).

up a competition between OH driven gas-phase chemistry that yields OCS and multiphase chemistry that likely suppresses OCS production from HPMTF. Here, we assume that the condensed phase chemistry of HPMTF, TFA, and TPA leads to sulfate (SO_4^{2-}) formation, although the condensed-phase chemistry of these intermediates is currently unknown and could lead to aqueous OCS production. To assess the impact of multiphase chemistry on OCS production from HPMTF, we utilize the entrainment-limited cloud loss parameterization developed by Holmes et al. (2019). As discussed in G. A. Novak et al. (2021), we find that multiphase chemistry has an irreversible and significant impact on [HPMTF] suppressing OCS production. The addition of HPMTF multiphase chemistry reduces P_{OCS} from 680.1 to 52.9 Gg S yr^{-1} with the largest differences found in regions of high cloud cover at high latitudes (Eastman et al., 2011; King et al., 2013; Figure 3a). When compared to the fixed yield approach (Figures 4a and 4b), P_{OCS} derived from the HPMTF-based chemical mechanism (Figures 4c and 4d) is significantly lower in the Southern Ocean, where consistent cloud cover irreversibly sequesters HPMTF and limits OCS production. In all cases, the annual trend in P_{OCS} reflects seasonal differences in E_{DMS} and [•OH], where P_{OCS} peaks in January in the Southern Ocean, July in the North Atlantic, and nearly constant in the equatorial Pacific (Figure 3b). The meridional distribution of P_{OCS}, where P_{OCS} is largest in the tropics (Figure 3b**,** blue line), agrees qualitatively with the *a posteriori* marine OCS source found by Ma et al. (2021), which is markedly different than that derived from the fixed-yield approach (Figure 3b, green line).

Uncertainty in the marine OCS source has long hindered quantitative budget closure and obscured interpretation of historical trends in OCS (Campbell et al., 2017). Our study provides a critical constraint on the DMS-derived source of OCS, which previously was believed to account for over half of the marine OCS flux with CS_2 oxidation and direct emissions accounting for the residual marine sources. While this new work places a more concentrated source in the tropical oceans - consistent with the location of the expected missing OCS source (Berry et al., 2013) - the study suggests a smaller overall OCS flux from the ocean which is inconsistent with recent suggestions that this source has generally been underestimated in global budgets (Launois et al., 2015; Ma et al., 2021). Consequently, the work raises important questions on whether the magnitude of the other marine sources such as CS_2 and direct emissions (Lennartz et al., 2021) are underestimated as suggested by Launois et al. (2015), or whether the land sink is overestimated. While the global analysis presented here significantly advances the representation OCS production from DMS, further refinement of the marine OCS source term will require detailed laboratory studies of HPMTF oxidation in the gas and condensed phase and assessment of multiphase cloud chemistry in global models.

Conflict of Interest

The authors declare no conflicts of interest relevant to this study.

Data Availability Statement

Experimental and model outputs from chamber experiment and a list of differential equations used to generate the model outputs for the first and multi-generational mechanism are archived at http://digital.library.wisc.edu/1793/82416 on the MINDS@UW databasehttps://minds.wisconsin.edu/. The quantum chemical data is deposited under https://doi.org/10.26165/JUELICH-DATA/4JCZ9O. Version 12.9.2 of the GEOS-Chem global chemical transport model was used in this analysis and can be found at www.geos-chem.org.

Acknowledgments
This work was supported by the NSF Center for Aerosol Impacts on Chemistry of the Environment under Grant CHE 1801971. Charles H. Fite and Christopher D. Holmes acknowledge support by the Future Investigators in NASA Earth and Space Science and Technology program (80NSSC19K1368) and NASA New Investigator Program (NNX16AI57G).

References

Alam, M. S., Rickard, A. R., Camredon, M., Wyche, K. P., Carr, T., Hornsby, K. E., et al. (2013). Radical product yields from the ozonolysis of short chain alkenes under atmospheric boundary layer conditions. *The Journal of Physical Chemistry A*, *117*(47), 12468–12483. https://doi.org/10.1021/jp408745h

Alecu, I. M., Zheng, J., Zhao, Y., & Truhlar, D. G. (2010). Computational thermochemistry: Scale factor databases and scale factors for vibrational frequencies obtained from electronic model chemistries. *Journal of Chemical Theory and Computation*, *6*(9), 2872–2887. https://doi.org/10.1021/ct100326h

Anglada, J. M., Crehuet, R., & Francisco, J. S. (2016). The stability of α-hydroperoxyalkyl radicals. *Chemistry—A European Journal*, *22*(50), 18092–18100. https://doi.org/10.1002/chem.201604499

Arathala, P., Katz, M., & Musah, R. A. (2020). Reaction mechanism, energetics, and kinetics of the water-assisted thioformaldehyde + OH reaction and the fate of its product radical under tropospheric conditions. *Physical Chemistry Chemical Physics*, *22*(18), 10027–10042. https://doi.org/10.1039/D0CP00570C

Asaf, D., Rotenberg, E., Tatarinov, F., Dicken, U., Montzka, S. A., & Yakir, D. (2013). Ecosystem photosynthesis inferred from measurements of carbonyl sulfide flux. *Nature Geoscience*, *6*(3), 186–190. https://doi.org/10.1038/ngeo1730

Atkinson, R., Baulch, D. L., Cox, R. A., Crowley, J. N., Hampson, R. F., Hynes, R. G., et al. (2006). Evaluated kinetic and photochemical data for atmospheric chemistry: Volume II – Gas phase reactions of organic species. *Atmospheric Chemistry and Physics*, *6*(11), 3625–4055. https://doi.org/10.5194/acp-6-3625-2006

Barnes, I., Becker, K. H., & Patroescu, I. (1994). The tropospheric oxidation of dimethyl sulfide: A new source of carbonyl sulfide. *Geophysical Research Letters*, *21*(22), 2389–2392. https://doi.org/10.1029/94gl02499

Barnes, I., Becker, K. H., & Patroescu, I. (1996). FTIR product study of the OH initiated oxidation of dimethyl sulphide: Observation of carbonyl sulphide and dimethyl sulphoxide. *Atmospheric Environment*, *30*(10–11), 1805–1814. https://doi.org/10.1016/1352-2310(95)00389-4

Barnes, I., Hjorth, J., & Mihalapoulos, N. (2006). Dimethyl sulfide and dimethyl sulfoxide and their oxidation in the atmosphere. *Chemical Reviews*, *106*(3), 940–975. https://doi.org/10.1021/cr020529+

Barone, S. B., Turnipseed, A. A., & Ravishankara, A. R. (1996). Reaction of OH with dimethyl sulfide (DMS). 1. Equilibrium constant for OH + DMS reaction and the kinetics of the OH·DMS + O2reaction. *Journal of Physical Chemistry*, *100*(35), 14694–14702. https://doi.org/10.1021/jp960866k

Bartlett, R. J., & Purvis, G. D. (1978). Many-body perturbation theory, coupled-pair many-electron theory, and the importance of quadruple excitations for the correlation problem. *International Journal of Quantum Chemistry*, *14*(5), 561–581. https://doi.org/10.1002/qua.560140504

Berkelhammer, M., Alsip, B., Matamala, R., Cook, D., Whelan, M. E., Joo, E., et al. (2020). Seasonal evolution of canopy stomatal conductance for a prairie and maize field in the midwestern United States from continuous carbonyl sulfide fluxes. *Geophysical Research Letters*, *47*(6), e2019GL085652. https://doi.org/10.1029/2019gl085652

Berkelhammer, M., Asaf, D., Still, C., Montzka, S., Noone, D., Gupta, M., et al. (2014). Constraining surface carbon fluxes using in situ measurements of carbonyl sulfide and carbon dioxide. *Global Biogeochemical Cycles*, *28*(2), 161–179. https://doi.org/10.1002/2013GB004644

Berkelhammer, M., Steen-Larsen, H. C., Cosgrove, A., Peters, A. J., Johnson, R., Hayden, M., & Montzka, S. A. (2016). Radiation and atmospheric circulation controls on carbonyl sulfide concentrations in themarine boundary layer. *Journal of Geophysical Research*, *121*(21), 13113–13128. https://doi.org/10.1002/2016JD025437

Berndt, T., Scholz, W., Mentler, B., Fischer, L., Hoffmann, E. H., Tilgner, A., et al. (2019). Fast peroxy radical isomerization and OH recycling in the reaction of OH radicals with dimethyl sulfide. *The Journal of Physical Chemistry Letters*, *10*(21), 6478–6483. https://doi.org/10.1021/acs.jpclett.9b02567

Berry, J., Wolf, A., Campbell, J. E., Baker, I., Blake, N., Blake, D., et al. (2013). A coupled model of the global cycles of carbonyl sulfide and CO_2: A possible new window on the carbon cycle. *Journal of Geophysical Research: Biogeosciences*, *118*(2), 842–852. https://doi.org/10.1002/jgrg.20068

Bertram, T. H., Kimmel, J. R., Crisp, T. A., Ryder, O. S., Yatavelli, R. L. N., Thornton, J. A., et al. (2011). A field-deployable, chemical ionization time-of-flight mass spectrometer. *Atmospheric Measurement Techniques*, *4*(7), 1471–1479. https://doi.org/10.5194/amt-4-1471-2011

Brühl, C., Lelieveld, J., Crutzen, P. J., & Tost, H. (2012). The role of carbonyl sulfide as a source of stratospheric sulfate aerosol and its impact on climate. *Atmospheric Chemistry and Physics*, *12*(3), 1239–1253. https://doi.org/10.5194/acp-12-1239-2012

Butkovskaya, N. I., & Setser, D. W. (2021). Reactions of OH and OD radicals with simple thiols and sulfides studied by infrared chemiluminescence of isotopic water products: Reaction OH + CH_3SH revisited. *International Journal of Chemical Kinetics*, *53*(6), 702–715. https://doi.org/10.1002/kin.21475

Campbell, J. E., Berry, J. A., Seibt, U., Smith, S. J., Montzka, S. A., Launois, T., et al. (2017). Large historical growth in global terrestrial gross primary production. *Nature*, *544*(7648), 84–87. https://doi.org/10.1038/nature22030

Chen, J., Berndt, T., Møller, K. H., Lane, J. R., & Kjaergaard, H. G. (2021). Atmospheric fate of the CH_3SOO radical from the CH_3S + O_2 equilibrium. *The Journal of Physical Chemistry A*, *125*(40), 8933–8941. https://doi.org/10.1021/acs.jpca.1c06900

Chin, M., & Davis, D. D. (1993). Global sources and sinks of OCS and CS_2 and their distributions. *Global Biogeochemical Cycles*, *7*(2), 321–337. https://doi.org/10.1029/93GB00568

Claflin, M. S., Pagonis, D., Finewax, Z., Handschy, A. V., Day, D. A., Brown, W. L., et al. (2021). An in situ gas chromatograph with automatic detector switching between PTR- and EI-TOF-MS: Isomer-resolved measurements of indoor air. *Atmospheric Measurement Techniques*, *14*(1), 133–152. https://doi.org/10.5194/amt-14-133-2021

Creasey, D. J., Evans, G. E., Heard, D. E., & Lee, J. D. (2003). Measurements of OH and HO_2 concentrations in the Southern Ocean marine boundary layer. *Journal of Geophysical Research*, *108*(15), 1–12. https://doi.org/10.1029/2002jd003206

Crounse, J. D., Nielsen, L. B., Jørgensen, S., Kjaergaard, H. G., & Wennberg, P. O. (2013). Autoxidation of organic compounds in the atmosphere. *The Journal of Physical Chemistry Letters*, *4*(20), 3513–3520. https://doi.org/10.1021/jz4019207

Crutzen, P. J. (1976). The possible importance of CSO for the sulfate layer of the stratosphere. *Geophysical Research Letters*, *3*(2), 73–76. https://doi.org/10.1029/gl003i002p00073

Davidson, C., Amrani, A., & Angert, A. (2021). Tropospheric carbonyl sulfide mass balance based on direct measurements of sulphur isotopes. *Proceedings of the National Academy of Sciences of the United States of America*, *118*(6), 1–6. https://doi.org/10.1073/pnas.2020060118

Devai, I., & DeLaune, R. D. (1995). Formation of volatile sulfur compounds in salt marsh sediment as influenced by soil redox condition. *Organic Geochemistry*, *23*(4), 283–287. https://doi.org/10.1016/0146-6380(95)00024-9

Donahue, N. M., Kroll, J. H., Anderson, J. G., & Demerjian, K. L. (1998). Direct observation of OH production from the ozonolysis of olefins. *Geophysical Research Letters*, *25*(1), 59–62. https://doi.org/10.1029/97GL53560

Dunning, T. H. (1989). Gaussian basis sets for use in correlated molecular calculations. I. The atoms boron through neon and hydrogen. *The Journal of Chemical Physics*, *90*(2), 1007–1023. https://doi.org/10.1063/1.456153

Dunning, T. H., Peterson, K. A., & Wilson, A. K. (2001). Gaussian basis sets for use in correlated molecular calculations. X. The atoms aluminium through argon revisited. *The Journal of Chemical Physics*, *114*(21), 9244–9253. https://doi.org/10.1063/1.1367373

Eastman, R., Warren, S. G., & Hahn, C. J. (2011). Variations in cloud cover and cloud types over the Ocean from surface observations, 1954–2008. *Journal of Climate*, *24*(22), 5914–5934. https://doi.org/10.1175/2011JCLI3972.1

Eckart, C. (1930). The penetration of a potential barrier by electrons. *Physical Review*, *35*(11), 1303–1309. https://doi.org/10.1103/PhysRev.35.1303

Estep, M. L., Moore, K. B., III, & Schaefer, H. F., III. (2020). Assessing the viability of the methylsulfinyl radical-ozone reaction. *Chem Phys Chem*, *21*(12), 1289–1294. https://doi.org/10.1002/cphc.202000188

Gelaro, R., McCarty, W., Suárez, M. J., Todling, R., Molod, A., Takacs, L., et al. (2017). The modern-era retrospective analysis for Research and applications, version 2 (MERRA-2). *Journal of Climate*, *30*(14), 5419–5454. https://doi.org/10.1175/JCLI-D-16-0758.1

Goerigk, L., Hansen, A., Bauer, C., Ehrlich, S., Najibi, A., & Grimme, S. (2017). A look at the density functional theory zoo with the advanced GMTKN55 database for general main group thermochemistry{,} kinetics and noncovalent interactions. *Physical Chemistry Chemical Physics*, *19*(48), 32184–32215. https://doi.org/10.1039/C7CP04913G

Grimme, S., Ehrlich, S., & Goerigk, L. (2011). Effect of the damping function in dispersion corrected density functional theory. *Journal of Computational Chemistry*, *32*(7), 1456–1465. https://doi.org/10.1002/jcc.21759

Hao, Y., Pan, X., Song, L., Ding, Y., Xia, W., Wang, S., et al. (2017). Anharmonic effect of the rate constant of the reactions of CH_3SCH_2OO system in high-temperature combustion. *Canadian Journal of Chemistry*, *95*(10), 1064–1072. https://doi.org/10.1139/cjc-2017-0216

Hoffmann, E. H., Tilgner, A., Schrödner, R., Bräuer, P., Wolke, R., & Herrmann, H. (2016). An advanced modeling study on the impacts and atmospheric implications of multiphase dimethyl sulfide chemistry. *Proceedings of the National Academy of Sciences of the United States of America*, *113*(42), 11776–11781. https://doi.org/10.1073/pnas.1606320113

Holmes, C. D., Bertram, T. H., Confer, K. L., Graham, K. A., Ronan, A. C., Wirks, C. K., & Shah, V. (2019). The role of clouds in the tropospheric NOx cycle: A new modeling approach for cloud chemistry and its global implications. *Geophysical Research Letters*, *46*(9), 4980–4990. https://doi.org/10.1029/2019GL081990

Hynes, A. J., Wine, P. H., & Nicovich, J. M. (1988). Kinetics and mechanism of the reaction of hydroxyl with carbon disulfide under atmospheric conditions. *The Journal of Physical Chemistry A*, *92*(13), 3846–3852. https://doi.org/10.1021/j100324a034

Iyer, S., Lopez-Hilfiker, F., Lee, B. H., Thornton, J. A., & Kurtén, T. (2016). Modeling the detection of organic and inorganic compounds using iodide-based chemical ionization. *The Journal of Physical Chemistry A*, *120*(4), 576–587. https://doi.org/10.1021/acs.jpca.5b09837

Jenkin, M. E., Hayman, G. D., Wellington, T. J., Hurley, M. D., Ball, J. C., Nielsen, O. J., & Ellermann, T. (1993). Kinetic and mechanistic study of the self reaction of $CH_3OCH_2O_2$ radicals at room temperature. *Journal of Physical Chemistry*, *97*(45), 11712–11723. https://doi.org/10.1021/j100147a027

Jenkin, M. E., Saunders, S. M., & Pilling, M. J. (1997). The tropospheric degradation of volatile organic compounds: A protocol for mechanism development. *Atmospheric Environment*, *31*(1), 81–104. https://doi.org/10.1016/S1352-2310(96)00105-7

Jenkin, M. E., Wyche, K. P., Evans, C. J., Carr, T., Monks, P. S., Alfarra, M. R., et al. (2012). Development and chamber evaluation of the MCM v3.2 degradation scheme for β-caryophyllene. *Atmospheric Chemistry and Physics*, *12*(11), 5275–5308. https://doi.org/10.5194/acp-12-5275-2012

Johnson, M. T. (2010). A numerical scheme to calculate temperature and salinity dependent air-water transfer velocities for any gas. *Ocean Science*, *6*(4), 913–932. https://doi.org/10.5194/os-6-913-2010

Johnston, H. S., & Heicklen, J. (1962). Tunneling corrections for unsymmetrical Eckart potential energy barriers. https://doi.org/10.1021/j100809a040

Jørgensen, S., & Kjaergaard, H. G. (2010). Effect of hydration on the hydrogen abstraction reaction by HO in DMS and its oxidation products. *The Journal of Physical Chemistry A*, *114*(14), 4857–4863. https://doi.org/10.1021/jp910202n

Kettle, A. J., Kuhn, U., Von Hobe, M., Kesselmeier, J., & Andreae, M. O. (2002). Global budget of atmospheric carbonyl sulfide: Temporal and spatial variations of the dominant sources and sinks. *Journal of Geophysical Research*, *107*(22), 1–16. https://doi.org/10.1029/2002JD002187

Khan, M. A. H., Bannan, T. J., Holland, R., Shallcross, D. E., Archibald, A. T., Matthews, E., et al. (2021). Impacts of hydroperoxymethyl thioformate on the global marine sulfur budget. *ACS Earth and Space Chemistry*, *5*(10), 2577–2586. https://doi.org/10.1021/acsearthspacechem.1c00218

King, M. D., Platnick, S., Menzel, W. P., Ackerman, S. A., & Hubanks, P. A. (2013). Spatial and temporal distribution of clouds observed by MODIS onboard the terra and aqua satellites. *IEEE Transactions on Geoscience and Remote Sensing*, *51*(7), 3826–3852. https://doi.org/10.1109/tgrs.2012.2227333

Krechmer, J., Lopez-Hilfiker, F., Koss, A., Hutterli, M., Stoermer, C., Deming, B., et al. (2018). Evaluation of a new reagent-ion source and focusing ion-molecule reactor for use in proton-transfer-reaction mass spectrometry. *Analytical Chemistry*, *90*(20), 12011–12018. https://doi.org/10.1021/acs.analchem.8b02641

Krechmer, J. E., Day, D. A., & Jimenez, J. L. (2020). Always lost but never forgotten: Gas-phase wall losses are important in all teflon environmental chambers. *Environmental Science and Technology*, *54*(20), 12890–12897. https://doi.org/10.1021/acs.est.0c03381

Krechmer, J. E., Pagonis, D., Ziemann, P. J., & Jimenez, J. L. (2016). Quantification of gas-wall partitioning in teflon environmental chambers using rapid bursts of low-volatility oxidized species generated in situ. *Environmental Science and Technology*, *50*(11), 5757–5765. https://doi.org/10.1021/acs.est.6b00606

Kremser, S., Thomason, L. W., von Hobe, M., Hermann, M., Deshler, T., Timmreck, C., et al. (2016). Stratospheric aerosol—observations, processes, and impact on climate. *Reviews of Geophysics*, *54*(2), 278–335. https://doi.org/10.1002/2015rg000511

Lana, A., Bell, T. G., Simó, R., Vallina, S. M., Ballabrera-Poy, J., Kettle, A. J., et al. (2011). An updated climatology of surface dimethlysulphide concentrations and emission fluxes in the global ocean. *Global Biogeochemical Cycles*, *25*(1), 1–n. https://doi.org/10.1029/2010GB003850

Launois, T., Belviso, S., Bopp, L., Fichot, C. G., & Peylin, P. (2015). A new model for the global biogeochemical cycle of carbonyl sulfide—Part 1: Assessment of direct marine emissions with an oceanic general circulation and biogeochemistry model. *Atmospheric Chemistry and Physics*, *15*(5), 2295–2312. https://doi.org/10.5194/acp-15-2295-2015

Lawson, S. J., Law, C. S., Harvey, M. J., Bell, T. G., Walker, C. F., Bruyn, D., et al. (2020). Methanethiol, dimethyl sulfide and acetone over biologically productive waters in the southwest Pacific Ocean. *Atmospheric Chemistry and Physics*, *20*(5), 3061–3078. https://doi.org/10.5194/acp-20-3061-2020

Lee, J. D., Moller, S. J., Read, K. A., Lewis, A. C., Mendes, L., & Carpenter, L. J. (2009). Year-round measurements of nitrogen oxides and ozone in the tropical North Atlantic marine boundary layer. *Journal of Geophysical Research*, *114*. https://doi.org/10.1029/2009jd011878

Lennartz, S. T., Gauss, M., von Hobe, M., & Marandino, C. A. (2021). Monthly resolved modelled oceanic emissions of carbonyl sulfide and carbon disulfide for the period 2000–2019. *Earth System Science Data*, *13*(5), 2095–2110. https://doi.org/10.5194/essd-13-2095-2021

Lester, M. I., & Klippenstein, S. J. (2018). Unimolecular decay of criegee intermediates to OH radical products: Prompt and thermal decay processes. *Accounts of Chemical Research*, *51*(4), 978–985. https://doi.org/10.1021/acs.accounts.8b00077

Ma, J., Kooijmans, L. M. J., Cho, A., Montzka, S. A., Glatthor, N., Worden, J. R., et al. (2021). Inverse modelling of carbonyl sulfide: Implementation, evaluation and implications for the global budget. *Atmospheric Chemistry and Physics*, *21*(5), 3507–3529. https://doi.org/10.5194/acp-21-3507-2021

Mardyukov, A., & Schreiner, P. R. (2018). Atmospherically relevant radicals derived from the oxidation of dimethyl sulfide. *Accounts of Chemical Research*, *51*(2), 475–483. https://doi.org/10.1021/acs.accounts.7b00536

Martínez, E., Albaladejo, J., Notario, A., & Jiménez, E. (2000). A study of the atmospheric reaction of CH_3S with O_3 as a function of temperature. *Atmospheric Environment*, *34*(29), 5295–5302. https://doi.org/10.1016/S1352-2310(00)00348-4

Martínez-Ávila, M., Peiró-García, J., Ramírez-Ramírez, V. M., & Nebot-Gil, I. (2003). Ab initio study on the mechanism of the $HCO+O_2 \rightarrow HO_2+CO$ reaction. *Chemical Physics Letters*, *370*(3), 313–318. https://doi.org/10.1016/S0009-2614(03)00106-4

Matsunaga, A., & Ziemann, P. J. (2010). Gas-wall partitioning of organic compounds in a teflon film chamber and potential effects on reaction product and aerosol yield measurements. *Aerosol Science and Technology*, *44*(10), 881–892. https://doi.org/10.1080/02786826.2010.501044

McDuffie, E. E., Smith, S. J., O'Rourke, P., Tibrewal, K., Venkataraman, C., Marais, E. A., et al. (2020). A global anthropogenic emission inventory of atmospheric pollutants from sector - and fuel-specific sources (1970–2017): An application of the community emissions data system (CEDS). *Earth System Science Data*, *12*(4), 3413–3442. https://doi.org/10.5194/essd-12-3413-2020

Montzka, S. A., Calvert, P., Hall, B. D., Elkins, J. W., Conway, T. J., Tans, P. P., & Sweeney, C. S. (2007). On the global distribution, seasonality, and budget of atmospheric carbonyl sulfide (COS) and some similarities to CO_2. *Journal of Geophysical Research*, *112*(9), 1–15. https://doi.org/10.1029/2006JD007665

Nightingale, P. D., Malin, G., Law, C. S., Watson, A. J., Liss, P. S., Liddicoat, M. I., et al. (2000). In situ evaluation of air-sea gas exchange parameterizations using novel conservative and volatile tracers. *Global Biogeochemical Cycles*, *14*(1), 373–387. https://doi.org/10.1029/1999gb900091

Novak, G., Vermeuel, M., & Bertram, T. (2019). Simultaneous detection of ozone and nitrogen dioxide by oxygen anion chemical ionization mass spectrometry: A fast time response sensor suitable for eddy covariance measurements. *Atmospheric Measurement Techniques Discussions*, *1*, 1–41. https://doi.org/10.5194/amt-2019-445

Novak, G. A., Fite, C. H., Holmes, C. D., Veres, P. R., Neuman, J. A., Faloona, I., et al. (2021). Rapid cloud removal of dimethyl sulfide oxidation products limits SO_2 and cloud condensation nuclei production in the marine atmosphere. *Proceedings of the National Academy of Sciences*, *118*(42), e2110472118. https://doi.org/10.1073/pnas.2110472118

Nozière, B., & Vereecken, L. (2019). Direct observation of aliphatic peroxy radical autoxidation and water effects: An experimental and theoretical study. *Angewandte Chemie International Edition*, *58*(39), 13976–13982. https://doi.org/10.1002/anie.201907981

Orlando, J. J., Tyndall, G. S., Vereecken, L., & Peeters, J. (2000). The atmospheric chemistry of the acetonoxy radical. *The Journal of Physical Chemistry A*, *104*(49), 11578–11588. https://doi.org/10.1021/jp0026991

Orlando, J. J., Tyndall, G. S., & Wallington, T. J. (2003). The atmospheric chemistry of alkoxy radicals. *Chemical Reviews*, *103*(12), 4657–4690. https://doi.org/10.1021/cr020527p

Pankow, J. F., & Asher, W. E. (2008). SIMPOL.1: A simple group contribution method for predicting vapor pressures and enthalpies of vaporization of multifunctional organic compounds. *Atmospheric Chemistry and Physics*, *8*(10), 2773–2796. https://doi.org/10.5194/acp-8-2773-2008

Patroescu, I. V., Barnes, I., & Becker, K. H. (1996). FTIR kinetic and mechanistic study of the atmospheric chemistry of methyl thiolformate. *Journal of Physical Chemistry*, *100*(43), 17207–17217. https://doi.org/10.1021/jp961452u

Randerson, J. T., Van Der Werf, G. R., Giglio, L., Collatz, G. J., & Kasibhatla, P. S. (2017). Global fire emissions database, version 4.1 (GFEDv4). ORNL distributed active archive center. https://doi.org/10.3334/ORNLDAAC/1293

Rickly, P. S., Xu, L., Crounse, J. D., Wennberg, P. O., & Rollins, A. W. (2021). Improvements to a laser-induced fluorescence instrument for measuring SO_2-Impact on accuracy and precision. *Atmospheric Measurement Techniques*, *14*(3), 2429–2439. https://doi.org/10.5194/amt-14-2429-2021

Rienstra-Kiracofe, J. C., Allen, W. D., & Schaefer, H. F. (2000). The $C_2H_5 + O_2$ reaction Mechanism: High-level ab initio characterizations. *The Journal of Physical Chemistry A*, *104*(44), 9823–9840. https://doi.org/10.1021/jp001041k

Rollins, A. W., Thornberry, T. D., Ciciora, S. J., McLaughlin, R. J., Watts, L. A., Hanisco, T. F., et al. (2016). A laser-induced fluorescence instrument for aircraft measurements of sulfur dioxide in the upper troposphere and lower stratosphere. *Atmospheric Measurement Techniques*, *9*(9), 4601–4613. https://doi.org/10.5194/amt-9-4601-2016

Saunders, S. M., Jenkin, M. E., Derwent, R. G., & Pilling, M. J. (2003). Protocol for the development of the Master Chemical Mechanism, MCM v3 (Part A): Tropospheric degradation of non-aromatic volatile organic compounds. *Atmospheric Chemistry and Physics*, *3*(1), 161–180. https://doi.org/10.5194/acp-3-161-2003

Solomon, S., Garcia, R. R., Rowland, F. S., & Wuebbles, D. J. (1986). On the depletion of Antarctic ozone. *Nature*, *321*(6072), 755–758. https://doi.org/10.1038/321755a0

Song, X., Hou, H., & Wang, B. (2005). Mechanistic and kinetic study of the $O + CH_3OCH_2$ reaction and the unimolecular decomposition of CH_3OCH_2O. *Physical Chemistry Chemical Physics*, *7*(23), 3980–3988. https://doi.org/10.1039/B510459A

The International GEOS-Chem User Community. (2020). Geoschem/geos-chem: GEOS-Chem 12.9.2 (12.9.2). https://doi.org/10.5281/zenodo.3959279

Van Rooy, P., Purvis-Roberts, K. L., Silva, P. J., Nee, M. J., & Cocker, D. (2021). Characterization of secondary products formed through oxidation of reduced sulfur compounds. *Atmospheric Environment*, *256*, 118148. https://doi.org/10.1016/j.atmosenv.2020.118148

Vaughan, S., Ingham, T., Whalley, L. K., Stone, D., Evans, M. J., Read, K. A., et al. (2012). Seasonal observations of OH and HO2in the remote tropical marine boundary layer. *Atmospheric Chemistry and Physics*, *12*(4), 2149–2172. https://doi.org/10.5194/acp-12-2149-2012

Vereecken, L., Carlsson, P. T. M., Novelli, A., Bernard, F., Brown, S. S., Cho, C., et al. (2021). Theoretical and experimental study of peroxy and alkoxy radicals in the NO_3-initiated oxidation of isoprene. *Physical Chemistry Chemical Physics*, *23*(9), 5496–5515. https://doi.org/10.1039/D0CP06267G

Vereecken, L., Huyberechts, G., & Peeters, J. (1997). Stochastic simulation of chemically activated unimolecular reactions. *The Journal of Chemical Physics*, *106*(16), 6564–6573. https://doi.org/10.1063/1.473656

Vereecken, L., Nguyen, T. L., Hermans, I., & Peeters, J. (2004). Computational study of the stability of α-hydroperoxyl- or α-alkylperoxyl substituted alkyl radicals. *Chemical Physics Letters*, *393*(4), 432–436. https://doi.org/10.1016/j.cplett.2004.06.076

Vereecken, L., & Nozière, B. (2020). H migration in peroxy radicals under atmospheric conditions. *Atmospheric Chemistry and Physics*, *20*(12), 7429–7458. https://doi.org/10.5194/acp-20-7429-2020

Vereecken, L., & Peeters, J. (1999). Theoretical investigation of the role of intramolecular hydrogen bonding in β-hydroxyethoxy and β-hydroxyethylperoxy radicals in the tropospheric oxidation of ethene. *The Journal of Physical Chemistry A*, *103*(12), 1768–1775. https://doi.org/10.1021/jp9826930

Vereecken, L., & Peeters, J. (2003). The 1,5-H-shift in 1-butoxy: A case study in the rigorous implementation of transition state theory for a multirotamer system. *The Journal of Chemical Physics*, *119*(10), 5159–5170. https://doi.org/10.1063/1.1597479

Vereecken, L., & Peeters, J. (2009). Decomposition of substituted alkoxy radicals—Part I: A generalized structure–activity relationship for reaction barrier heights. *Physical Chemistry Chemical Physics*, *11*(40), 9062–9074. https://doi.org/10.1039/B909712K

Vereecken, L., & Peeters, J. (2010). A structure–activity relationship for the rate coefficient of H-migration in substituted alkoxy radicals. *Physical Chemistry Chemical Physics*, *12*(39), 12608–12620. https://doi.org/10.1039/C0CP00387E

Vereecken, L., Peeters, J., Orlando, J. J., Tyndall, G. S., & Ferronato, C. (1999). Decomposition of β-hydroxypropoxy radicals in the OH-initiated oxidation of propene. A theoretical and experimental study. *The Journal of Physical Chemistry A*, *103*(24), 4693–4702. https://doi.org/10.1021/jp990046i

Vereecken, L., Vu, G., Wahner, A., Kiendler-Scharr, A., & Nguyen, H. M. T. (2021). A structure activity relationship for ring closure reactions in unsaturated radicals. *Physical Chemistry Chemical Physics*, *23*(31), 16564–16576. https://doi.org/10.1039/D1CP02758A

Veres, P. R., Andrew Neuman, J., Bertram, T. H., Assaf, E., Wolfe, G. M., Williamson, C. J., et al. (2020). Global airborne sampling reveals a previously unobserved dimethyl sulfide oxidation mechanism in the marine atmosphere. *Proceedings of the National Academy of Sciences of the United States of America*, *117*(9), 4505–4510. https://doi.org/10.1073/pnas.1919344117

Vermeuel, M. P., Novak, G. A., Jernigan, C. M., & Bertram, T. H. (2020). Diel profile of hydroperoxymethyl thioformate: Evidence for surface deposition and multiphase chemistry. *Environmental Science and Technology*, *54*(19), 12521–12529. https://doi.org/10.1021/acs.est.0c04323

Von Hobe, M., Cutter, G. A., Kettle, A. J., & Andreae, M. O. (2001). Dark production: A significant source of oceanic COS. *Journal of Geophysical Research*, *106*(C12), 31217–31226. https://doi.org/10.1029/2000jc000567

Wang, X., Jacob, D. J., Downs, W., Zhai, S., Zhu, L., Shah, V., et al. (2021). Global tropospheric halogen (Cl, Br, I) chemistry and its impact on oxidants. *Atmospheric Chemistry and Physics*, *21*(18), 13973–13996. https://doi.org/10.5194/acp-21-13973-2021

Wang, X., Jacob, D. J., Eastham, S. D., Sulprizio, M. P., Zhu, L., Chen, Q., et al. (2019). The role of chlorine in global tropospheric chemistry. *Atmospheric Chemistry and Physics*, *19*(6), 3981–4003. https://doi.org/10.5194/acp-19-3981-2019

Watts, S. F. (2000). The mass budgets of carbonyl sulfide, dimethyl sulfide, carbon disulfide and hydrogen sulfide. *Atmospheric Environment*, *34*(5), 761–779. https://doi.org/10.1016/S1352-2310(99)00342-8

Werle, P., Mücke, R., & Slemr, F. (1993). The limits of signal averaging in atmospheric trace-gas monitoring by tunable diode-laser absorption spectroscopy (TDLAS). *Applied Physics B Photophysics and Laser Chemistry*, *57*(2), 131–139. https://doi.org/10.1007/BF00425997

Wine, P. H., Thompson, R. J., & Semmes, D. H. (1984). Kinetics of OH reactions with aliphatic thiols. *International Journal of Chemical Kinetics*, *16*(12), 1623–1636. https://doi.org/10.1002/kin.550161215

Wolfe, G. M., Marvin, M. R., Roberts, S. J., Travis, K. R., & Liao, J. (2016). The framework for 0-D atmospheric modeling (F0AM) v3.1. *Geoscientific Model Development*, *9*(9), 3309–3319. https://doi.org/10.5194/gmd-9-3309-2016

Wu, R., Wang, S., & Wang, L. (2015). New mechanism for the atmospheric oxidation of dimethyl sulfide. The importance of intramolecular hydrogen shift in a CH_3SCH_2OO radical. *The Journal of Physical Chemistry A*, *119*(1), 112–117. https://doi.org/10.1021/jp511616j

Ye, Q., Goss, M. B., Isaacman-VanWertz, G., Zaytsev, A., Massoli, P., Lim, C., et al. (2021). Organic sulfur products and peroxy radical isomerization in the OH oxidation of dimethyl sulfide. *ACS Earth and Space Chemistry*. https://doi.org/10.1021/acsearthspacechem.1c00108

Yin, F., Grosjean, D., Flagan, R. C., & Seinfeld, J. H. (1990). Photooxidation of dimethyl sulfide and dimethyl disulfide. II: Mechanism evaluation. *Journal of Atmospheric Chemistry*, *11*(4), 365–399. https://doi.org/10.1007/BF00053781

Yin, F., Grosjean, D., & Seinfeld, J. H. (1990). Photooxidation of dimethyl sulfide and dimethyl disulfide. I: Mechanism development. *Journal of Atmospheric Chemistry*, *11*(4), 309–364. https://doi.org/10.1007/BF00053780

Zhao, Y., & Truhlar, D. G. (2008). The M06 suite of density functionals for main group thermochemistry, thermochemical kinetics, noncovalent interactions, excited states, and transition elements: Two new functionals and systematic testing of four M06-class functionals and 12 other function. *Theoretical Chemistry Accounts*, *120*(1), 215–241. https://doi.org/10.1007/s00214-007-0310-x

Zhu, L., & Bozzelli, J. W. (2006). Kinetics of the multichannel reaction of methanethiyl radical ($CH_3S\bullet$) with $3O_2$. *The Journal of Physical Chemistry A*, *110*(21), 6923–6937. https://doi.org/10.1021/jp056209m

Zumkehr, A., Hilton, T. W., Whelan, M., Smith, S., Kuai, L., Worden, J., & Campbell, J. E. (2018). Global gridded anthropogenic emissions inventory of carbonyl sulfide. *Atmospheric Environment*, *183*, 11–19. https://doi.org/10.1016/j.atmosenv.2018.03.063